

Research and Development for Thermoelectric Generation Technology Using Waste Heat from Steelmaking Process

TAKASHI KUROKI,^{1,3} RYOTA MURAI,¹ KAZUYA MAKINO,²
KOUJI NAGANO,² TAKESHI KAJIHARA,² HIROMASA KAIBE,²
HIROKUNI HACHIUMA,² and HIDETOSHI MATSUNO¹

1.—Environmental Process Research Department Steel Research Laboratory, JFE Steel Corporation, 1-1, Minamiwataridacho, Kawasaki-ku, Kawasaki, Kanagawa 210-0855, Japan.
2.—Thermo Generation Business Development Division, KELK Ltd., 3-25-1 Shinomiya, Hiratsuka, Kanagawa 254-8543, Japan. 3.—e-mail: ta-kuroki@jfe-steel.co.jp

In Japan, integrated steelworks have greatly lowered their energy use over the past few decades through investment in energy-efficient processes and facilities, maintaining the highest energy efficiency in the world. However, in view of energy security, the steelmaking industry is strongly required to develop new technologies for further energy saving. Waste heat recovery can be one of the key technologies to meet this requirement. To recover waste heat, particularly radiant heat from steel products which has not been used efficiently yet, thermoelectric generation (TEG) is one of the most effective technologies, being able to convert heat directly into electric power. JFE Steel Corporation (JFE) implemented a 10-kW-class grid-connected TEG system for JFE's continuous casting line with KELK Ltd. (KELK), and started verification tests to generate electric power using radiant heat from continuous casting slab at the end of fiscal year 2012. The TEG system has 56 TEG units, each containing 16 TEG modules. This paper describes the performance and durability of the TEG system, which has been investigated under various operating conditions at the continuous casting line.

Key words: Exhaust heat, heat recovery, thermoelectric generation system

INTRODUCTION

Waste heat recovery is one of the approaches that will play an important role in the future. To recover waste heat, particularly radiant heat from steel products which has not been used efficiently yet, thermoelectric generation (TEG) is one of the most effective technologies, as such devices can convert heat directly into electricity. Their absence of mechanical moving parts, wide range of operating temperature, scalability, lack of CO₂ emissions during operation, and long lifetime make TEG attractive for energy generation applications.

JFE Steel Corporation (JFE) implemented a 10-kW-class grid-connected thermoelectric generation (TEG) system for JFE's continuous casting

line with KELK Ltd. (KELK), and started verification tests to generate electric power using radiant heat from continuous casting slab at the end of fiscal year 2012.¹ Figures 1 and 2 show an illustration and photograph of the TEG system installed at JFE's continuous casting line.

This paper describes the performance and durability of the TEG system, which have been investigated under various operating conditions at the continuous casting line.

THERMOELECTRIC GENERATION SYSTEM AT STEELWORKS

The TEG system has 56 TEG units, each containing 16 TEG modules, and the size of the TEG system is about 4 m × 2 m, with a distance between the slab and the TEG units of about 2 m. The heat

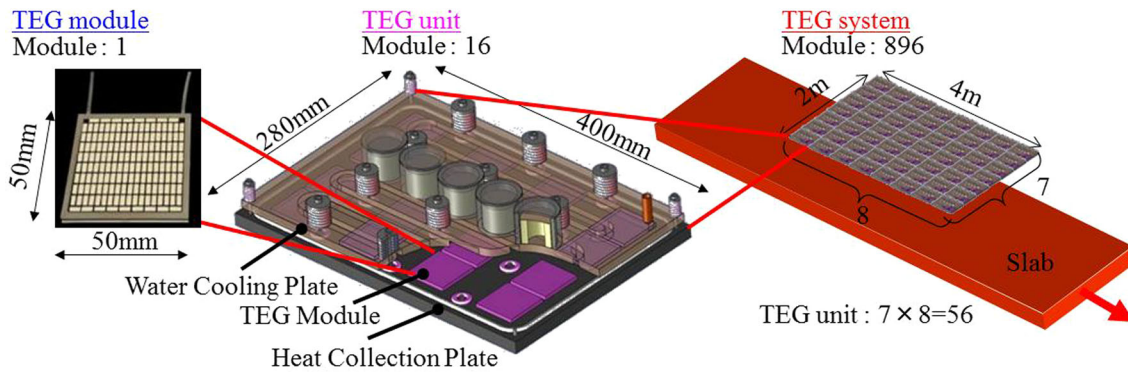


Fig. 1. Schematic illustration of TEG module, TEG unit, and TEG system.

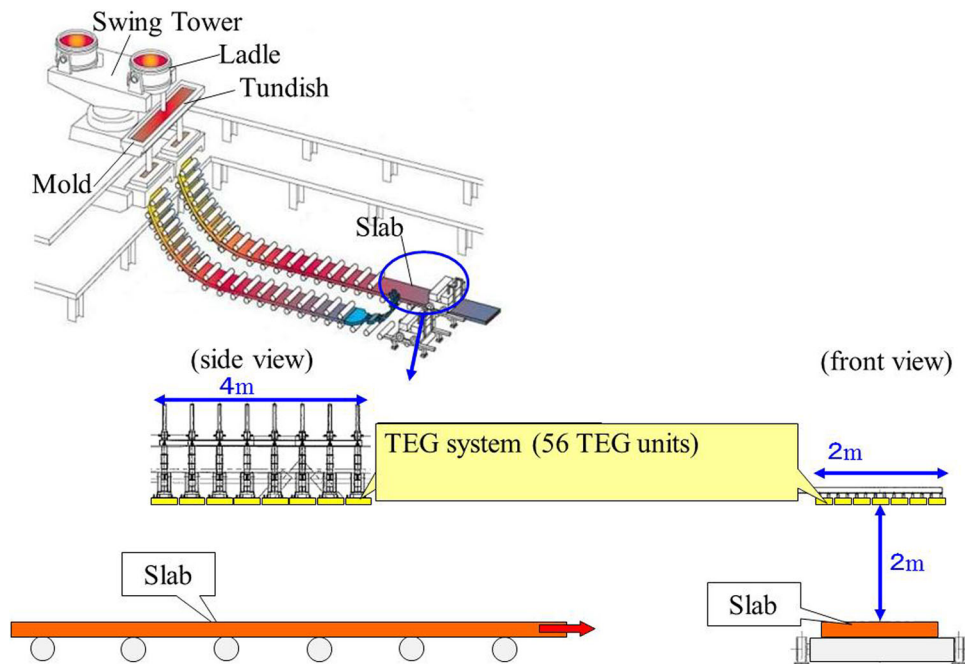


Fig. 2. Thermoelectric generation system installed at JFE's continuous casting line [East Japan Works (Keihin)].

collection plates of the TEG units were heated by radiant heat from continuous casting slab.

The bismuth telluride TEG modules, made of a number of n - and p -type thermoelectric elements, were developed by KELK, having maximum output power of 24 W and maximum conversion efficiency of 7.2%, for hot-side temperature of 553 K and cold-side temperature of 303 K. The maximum operating temperature is 553 K at the high-temperature side, with normal operation at 523 K or below, with a maximum of 423 K at the low-temperature side. The evaluation of the maximum output and conversion efficiency was carried out for a cold-side temperature of $T_c = 303$ K. The voltage V value at current $I = 0$, i.e., the open-circuit voltage V_o , was 12 V and 14 V for $T_h = 523$ K and 553 K, respectively. V decreases linearly with I , with a slope yielding the internal resistance R_i of the TEG module. R_i increases as T_h rises. In the case of $T_i = 553$ K, R_i is about 2 Ω . The

output P can be calculated from the external load r connected to the TEG module as $P = V \times I$. P reaches its maximum P_{\max} at impedance matching, when $R_i = r$. The maximum output was 18 W and 24 W for $T_h = 523$ K and 553 K, respectively.^{1,2}

A total of 16 TEG modules were connected in series in each TEG unit. Each TEG module was sandwiched between the heat collection plate and water cooling plate by a spring structure, meaning that an almost constant pressure was applied to the modules, even when a temperature difference was generated. The pressure was set as 1 MPa as a criterion, with a cooling water flow rate of 1.7×10^{-4} m³/s per TEG unit. The size of the heat collection plate was 400 mm \times 280 mm. Copper was used for the heat collection plate and water-cooled plate. The heat collection plate was blackened using surface treatment by electroless nickel plating to yield an emissivity of about 0.95.²

VERIFICATION TESTS

To evaluate the performance of the TEG system, we adopted an evaluation method using both experiment and simulation. Equations 1 and 2 are the basic equations of the TEG.

$$Q_a = \alpha_e T_{hj} I - \frac{1}{2} r_e I^2 + K_e \Delta T_j, \quad (1)$$

$$Q_d = \alpha_e T_{cj} I + \frac{1}{2} r_e I^2 + K_e \Delta T_j. \quad (2)$$

Here, heat Q_a is supplied by the thermal source at the hot surface, and Q_d is the heat flowing out at the cold surface. α_e is the Seebeck coefficient, r_e is the internal electrical resistance, and K_e is the thermal conductance. I represents the electric current.³ These equations are derived from the heat equation including the Seebeck effect and Joule heating with boundary conditions of the hot-side temperature (T_{hj}) and the cold-side temperature (T_{cj}).

The power generation output P_g is given by Eq. 3.

$$P_g = Q_a - Q_d = (\alpha_e \Delta T_j - r_e I) I = R_L I^2. \quad (3)$$

Here, R_L is the external electric resistance.

Also, when $r_e = R_L$, the maximum generation output P_{gmax} is given by Eq. 4.

$$P_{gmax} = \frac{1}{4} \cdot \frac{(\alpha_e \Delta T_j)^2}{r_e}. \quad (4)$$

Here, ΔT_j is the temperature difference $T_{hj} - T_{cj}$.

To obtain high power generation output, a large temperature difference ΔT_j is required. On the other hand, T_{hj} must remain below the maximum tolerated temperature of 553 K. Therefore, it is very important to simulate T_{hj} for various conditions. In this system, Q_a is mainly radiant heat from the slab. Q_a is expressed by Eq. 5.

$$Q_a = \varepsilon \cdot F \cdot \sigma \cdot A (T_s^4 - T_h^4) + h \cdot A \cdot \Delta T. \quad (5)$$

Here, ε is the emissivity, σ is the Stefan–Boltzmann constant, F is the view factor, T_s is the slab temperature, T_h is the hot-side temperature of the TEG unit, A is the area of the heat collection plate of the TEG unit, ΔT is the temperature difference between T_h and T_a (the ambient temperature), and h is the heat transfer coefficient. T_{hj} can be derived as a function of the view factor F of the system, the current I , and the thermal conductivity of the heat collection plate.

Using Eqs. 1–5, the temperature of the TEG unit and P_{gmax} were numerically investigated for several

experimental conditions. When the continuous casting line is in operation, the TEG units are warmed by radiant heat, a temperature difference is generated, and power is output by the TEG units. The view factor F depends on the orientation of the small areas dA_1 and dA_2 and the distance between them (r). F is given by Eq. 6.

$$F = \iint \frac{\cos \phi_1 \cos \phi_2}{A_1 \pi r^2} dA_1 dA_2, \quad (6)$$

where ϕ_1 and ϕ_2 are the angles between the unit normals to the areas and the line r connecting the two areas, as shown in Fig. 3.

The view factor F in Eq. 5 is a function of the slab width and the distance from the slab to the TEG units and is inversely proportional to the distance. So, the heat input Q_a becomes larger as the slab becomes wider. Therefore, the power output of the TEG units increases with the slab width. Figure 4 shows the simulated power output distribution of the TEG unit in the slab width direction as a function of slab width. The view factor changes with unit position or slab width, thus changing the power output.

Figure 5 shows the simulated power output distribution of the TEG unit in the slab width direction as a function of slab temperature. The heat input Q_a becomes larger when the slab temperature T_s rises. For greater heat input, the heat collection plate temperature rises and the temperature difference ΔT_j increases. Therefore, the power output of the TEG units increases with the slab temperature.

Figure 6 shows the simulation and some experimental results for the power output of the TEG units. The measurements of the power output of the TEG units seem to be similar to the simulated output when the slab temperature is 1158 K and the slab width is 1.5 m.

The durability of the TEG system was also investigated. Figure 7 shows the relationship between power output and time. The power output

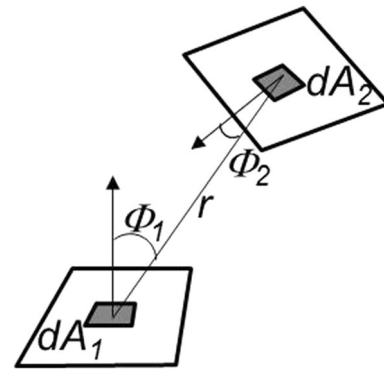


Fig. 3. Geometry for view factor definition.

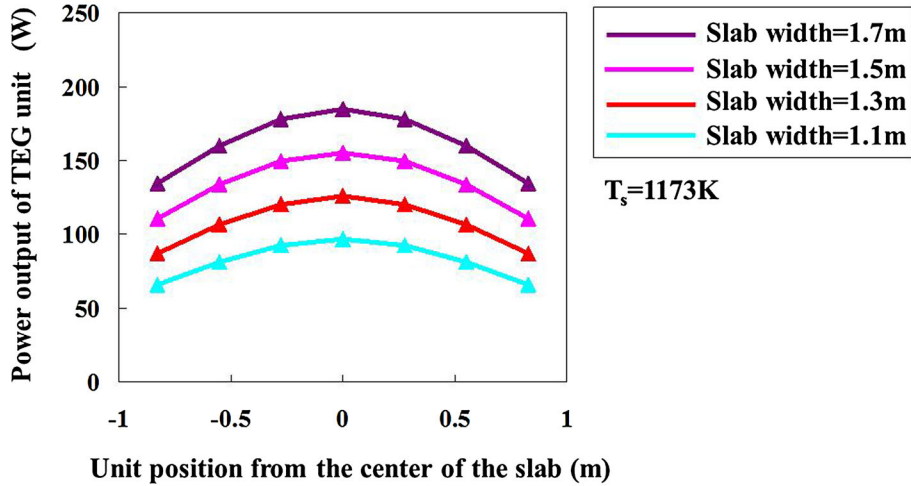


Fig. 4. Relationship between unit position and power output of TEG unit as a function of slab width.

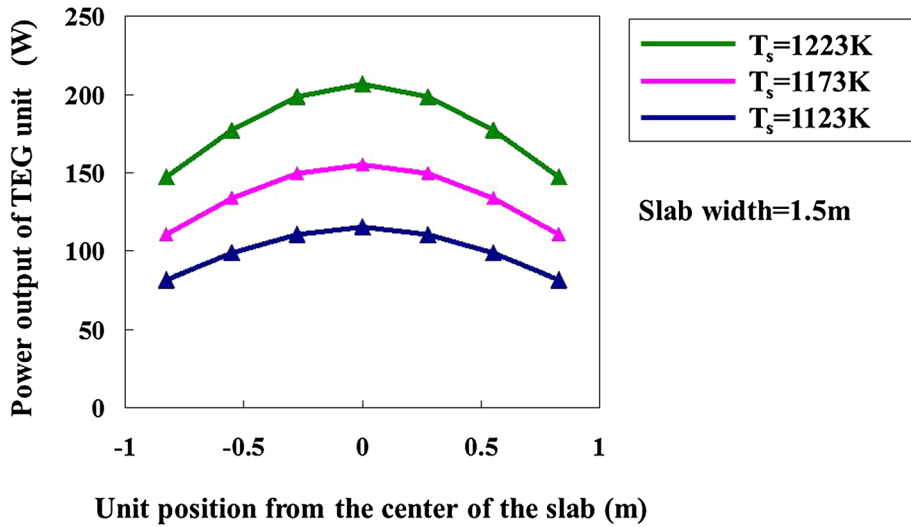


Fig. 5. Relationship between unit position and power output of TEG unit as a function of slab temperature.

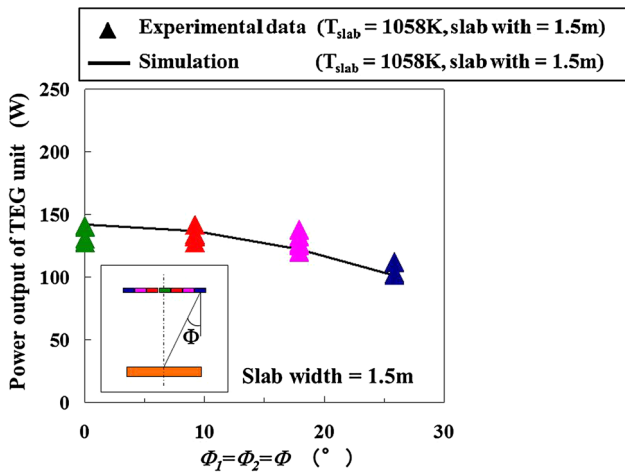


Fig. 6. Relationship between angle $\Phi(= \Phi_1 = \Phi_2)$ and power output of TEG unit.

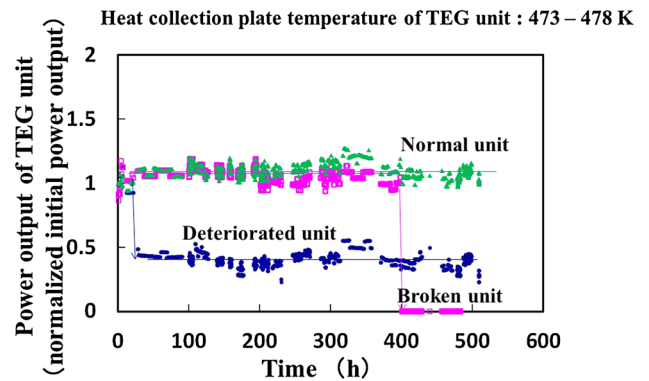


Fig. 7. Relationship between power output and time for some TEG units.

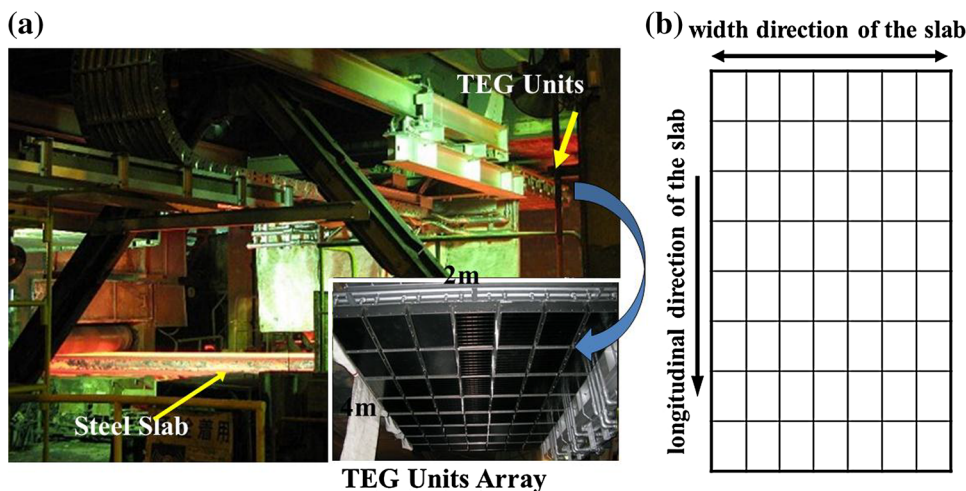


Fig. 8. (a) Photo of TEG unit array (b) Schematic illustration of TEG unit array.

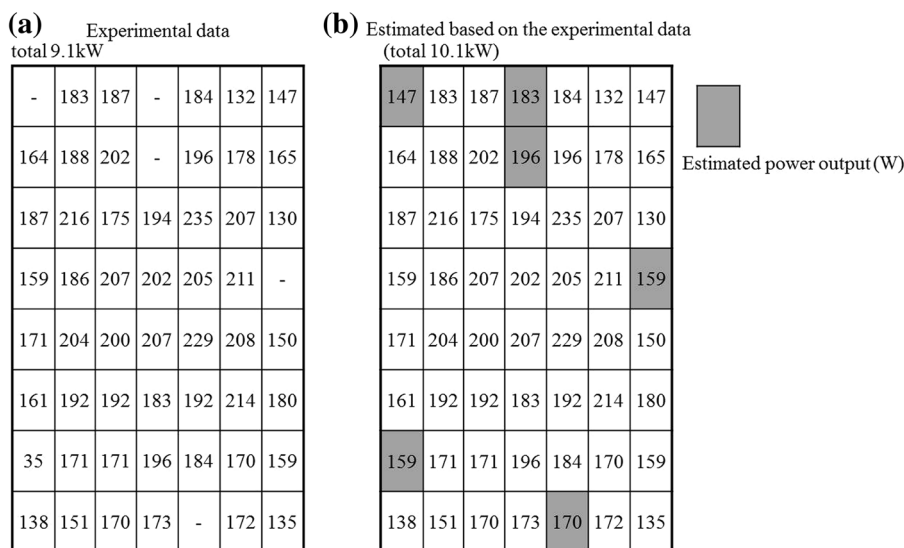


Fig. 9. Example power output of each TEG unit (slab width 1.6 m): (a) experimental data, and (b) estimated based on experimental data.

of most TEG units remained constant, but some TEG units were broken and the power output decreased. It became clear that it was necessary to improve the quality of the junction between the thermoelectric element and the electrode material.

Figure 8 shows a photo and schematic illustration of the TEG unit array. Figure 9 shows an example power output of each TEG unit for slab width of 1.6 m. The TEG system outputs about 9.1 kW. The system would show an output of 10.1 kW if broken or deteriorated units gave their normal output. Figure 10 shows the power output of the TEG units. The power output estimated based on the experimental data of the TEG units seems to be similar to the simulated output.

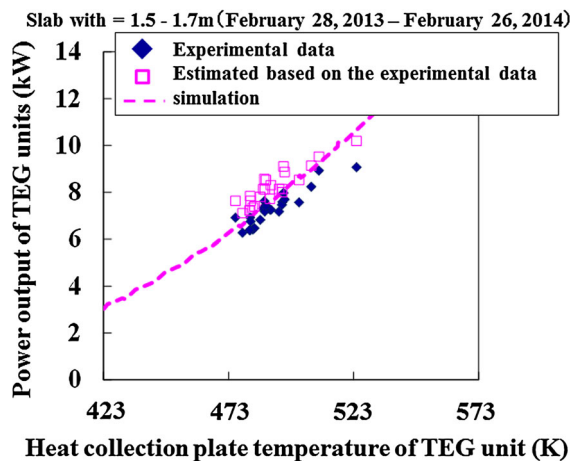


Fig. 10. Power output of TEG units.

CONCLUSIONS

The power output distribution of each TEG unit was simulated using the basic TEG equations and the view factor. We observed good agreement between the simulation and the experimental data.

ACKNOWLEDGEMENTS

This study was carried out as part of the New Energy and Industrial Technology Development Organization (NEDO) project “Research and

Development Program for Innovative Energy Efficiency Technology.”

REFERENCES

1. T. Kuroki, K. Kabeya, K. Makino, T. Kajihara, H. Kaibe, H. Hachiuma, H. Matsuno, and A. Fujibayashi, *J. Electron. Mater.* 43, 2405 (2014).
2. H. Kaibe, S.K. Makino, T. Kajihara, S. Fujimoto, and H. Hachiuma, *AIP Conf. Proc.* 1449, 524 (2012).
3. K. Uemura and I. Nishida, *Netsudenhandoutai to Sono Ouyou [A thermoelectric semiconductor and the application]* (Nikkan Kogyo Shinbunsha: Tokyo, 1988), p. 26.